SRI International

Annual Technical Status Report 2 • 8 March 1995
Covering the Period 1 April 1994 to 30 March 1995

Modeling of the Coupled Magnetospheric and Neutral Wind Dynamos

Submitted by:

Jeff P. Thayer, Research Physicist
Geoscience and Engineering Center

SRI Project 4604

Prepared for:

National Aeronautics and Space Administration
Goddard Space Flight Center
Greenbelt, Maryland 20771

Attn: Mary Mellott, Code: SS
NASA Technical Officer

Grant: NAGW-3508

Approved:

James F. Vickrey, Director
Geoscience and Engineering Center

333 Ravenswood Avenue • Menlo Park, CA 94025-3493 • (415) 326-6200 • FAX (415) 326-5512 • Telex 334486

1 INTRODUCTION

This annual report summarizes the progress made over the period April 1, 1994 to March 30, 1994, for NASA Grant No. NAGW-3508 entitled "Modeling of the Coupled Magnetospheric and Neutral Wind Dynamos." The main effort over this period concentrated on completing the modeling of the high-latitude Poynting flux and comparing these results with the DE-B measurements. The following summarizes this aspect of the research.

2 PROGRESS DURING THE REPORTING PERIOD

Work at SRI involved modeling the exchange of electromagnetic energy between the ionosphere and magnetosphere to help interpret the DE-B Poynting flux observations. To describe the electrical properties of the high-latitude ionosphere, we constructed a numerical model, from the framework provided by the Vector Spherical Harmonic (VSH) model, that determines the ionospheric currents, conductivities, and electric fields including both magnetospheric inputs and neutral wind dynamo effects. This model development grew from the earlier question of whether an electrical energy source in the ionosphere was capable of providing an upward Poynting flux. The model solves the steady-state neutral wind dynamo equations and the Poynting flux equation to provide insight into the electrodynamic role of the neutral winds.

The modeling effort to determine the high-latitude energy flux has been able to reproduce many of the large-scale features observed in the Poynting flux measurements made by DE-2. Because the Poynting flux measurement is an integrated result of energy flux into or out of the ionosphere, we investigated the ionospheric properties that may contribute to the observed flux of energy measured by the spacecraft. During steady state the electromagnetic energy flux, or DC Poynting flux, is equal to the Joule heating rate and the mechanical energy transfer rate in the high-latitude ionosphere. Although the Joule heating rate acts as an energy sink, transforming electromagnetic energy into thermal or internal energy of the gas, the mechanical energy transfer rate may be either a sink or source of electromagnetic energy. In the steady state, it is only the mechanical energy transfer rate that can generate electromagnetic energy and result in a DC Poynting flux that is directed out of the ionosphere.

The model simulation led to a number of conclusions.

- The electromagnetic energy flux is predominantly directed into the high-latitude ionosphere, with greater input in the morning sector than the evening sector by a factor of three.
- The Joule heating rate accounts for much of the electromagnetic energy deposited in the ionosphere, with the conductivity-weighted neutral wind contributing significantly to the Joule heating rate and thus to the net electromagnetic energy flux in the ionosphere.
- On average, the mechanical energy transfer rate contributes about 20% to the net electromagnetic energy flux in the dawn, dusk, and polar cap regions, acting as a sink of electromagnetic energy flux in the dawn and dusk sectors and a source of electromagnetic energy flux in the polar cap.
- An upward electromagnetic energy flux is found in the regions near the convection reversal boundaries. This flux is due to the mechanical energy transfer rate exceeding the Joule heating rate. The upward electromagnetic energy flux was found to be small partly due to the relationship of the conductivity-weighted neutral wind to the imposed electric field and partly due to the Joule heating rate increasing irrespective of the source of electromagnetic energy flux.

2.1 TRAVEL

There was no travel during this reporting period.

2.2 SUBCONTRACT

A subcontract to the University of Texas at Dallas (UTD) has been established and is under the direction of Professor Rod Heelis. During the reporting period, UTD has continued an examination of satellite measurements of the DC Poynting flux as an indicator of electromagnetic energy transport through the high latitude ionosphere.

2.3 SCIENTIFIC REPORTS

A paper describing the numerical results for the modeling study of the Poynting flux has been accepted and is in press: "Interpretation and Modeling of the High-Latitude Electromagnetic Energy Flux," by J.P. Thayer, J.F. Vickrey, J.B. Gary, and R.A. Heelis.

A paper describing the statistical distribution of the Poynting flux measurements from DE-2 has been accepted and is in press: "Summary of Field-Aligned Poynting Flux Observations From DE 2," by J.B. Gary, R.A. Heelis, and J.P. Thayer.

3 PLANS FOR THE COMING PERIOD

A number of aspects of this research will be addressed in the coming period. The neutral wind dynamo analysis will continue with further development in modeling the currents and/or electric fields under different geophysical conditions and for different seasons. A term analysis will also be carried out to describe the importance of each term in the dynamo equation under these different geophysical conditions. Further development of the spectral code is required to accommodate the latest version of the NCAR-TIEGCM. New model runs from the NCAR-TIEGCM are anticipated that will provide better tidal parameterization within the model and include a better electrodynamic simulation. Also, a better representation of the magnetosphere will be pursued in order to incorporate more realistic coupling between the ionosphere and magnetosphere.

The modeling of the electrical energy flux between the ionosphere and magnetosphere will be pursued further providing a new view and new insight into describing the role of the neutral wind dynamo in terms of its electrical energetics. This modeling effort will benefit from the dynamo calculations and will address similar issues.

Aspects of the numerical modeling will be compared with observed electrodynamic features from the DE-2 spacecraft in coordination with the UTD team. There is a close relationship between the Poynting flux measurements made by DE-2 and the neutral wind dynamo processes, as discussed in the papers appended to this report. We will be pursuing this line of study to help elucidate the electrodynamic processes involved in contributing to the observed Poynting flux measurements.

"Interpretation and Modeling of the High-Latitude Electromagnetic Energy Flux," by J.P. Thayer, J.F. Vickrey, J.B. Gary, and R.A. Heelis (in press).

Summary of Field-Aligned Poynting Flux
Observations From DE 2," by J.B. Gary,
R.A. Heelis, and J.P. Thayer (in press).

INTERPRETATION AND MODELING OF THE HIGH-LATITUDE ELECTROMAGNETIC ENERGY FLUX

J.P. Thayer and J.F. Vickrey

SRI International, Menlo Park, California

R.A. Heelis, and J.B. Gary

Center for Space Science, Physics Program, University of Texas at Dallas, Richardson

For submission to the *Journal of Geophysical Research*

February 1995

ABSTRACT

An interpretation of the electromagnetic energy flux at high latitudes under steady-state conditions is presented and analyzed through modeling of the large-scale coupling between the high-latitude ionosphere and magnetosphere. In this paper, we elucidate the steady-state relationship between the electromagnetic energy flux (divergence of the DC Poynting flux), the Joule heating rate and the mechanical energy transfer rate in the high-latitude ionosphere. We also demonstrate the important role of the neutral wind and its conductivity-weighted distribution with altitude in determining the resultant exchange of electromagnetic energy at high latitudes. Because the Poynting flux approach accounts for the neutral wind, implicitly, and describes the net electromagnetic energy flux between the magnetosphere and ionosphere, it is a fundamental measure of energy transfer in the system. A significant portion of this energy transfer results in Joule heating; however, the conversion of electromagnetic energy flux into mechanical energy of the neutrals is also considerable and can in some regions exceed the Joule heating rate. We will show that neglect of the neutral dynamics in calculations of the Joule heating rate can be misleading.

To evaluate and interpret the electromagnetic energy flux at high latitudes, we employ the Vector Spherical Harmonic model, which is based on the NCAR Thermosphere–Ionosphere General Circulation Model, to provide the steady-state properties of the thermosphere–ionosphere system under moderate to quiet geomagnetic activity. For the specific geophysical conditions modeled, we conclude that 1) the electromagnetic energy flux is predominantly directed into the high-latitude ionosphere with greater input in the morning sector than in the evening sector, as supported by DE-2 observations. 2) The Joule heating rate accounts for much of the electromagnetic energy deposited in the ionosphere, with the conductivity-weighted neutral wind contributing significantly to the Joule heating rate and thus affecting the net electromagnetic energy flux in the ionosphere. 3) On average, the mechanical energy transfer

rate amounts to about 10% to 30% of the net electromagnetic energy flux in the auroral dawn, dusk, and polar cap regions, acting as a sink of electromagnetic energy flux in the dawn and dusk sectors and a source in the polar cap. 4) Weak regions of upward electromagnetic energy flux are found near the convection reversal boundaries where the mechanical energy transfer rate exceeds the Joule heating rate. In general, large upward electromagnetic energy fluxes may be rare as the always positive Joule heating rate increases irrespective of the source of electromagnetic energy flux; i.e., neutral dynamics contribute directly to the Joule heating rate.

1 INTRODUCTION

The magnetosphere–ionosphere (M–I) system at high latitudes can exhibit a diverse character in the distribution of currents and electric fields and in the population and energy of plasma particles. These features help to define the various regions of the M–I system. These regions are coupled through the exchange of energy between the electromagnetic field and the plasma. The energy exchange involved in this process can be described in terms of Poynting's theorem,

$$\iiint_V \frac{\partial}{\partial t}\left(\frac{B^2}{2\mu_0} + \frac{\varepsilon_0}{2}E^2\right) dV + \iiint_V \frac{\nabla \circ \left(\vec{E} \times \vec{B}\right)}{\mu_0} dV + \iiint_V \vec{j} \circ \vec{E}\, dV = 0 \quad , \tag{1}$$

where the first term is the electromagnetic energy density within the volume, the second term is the divergence of the electromagnetic (Poynting) energy flux within the volume, and the third term is the volume energy transfer rate. The derivation of Poynting's theorem comes directly from Maxwell's equations using the identity $\nabla \circ \left(\vec{E} \times \vec{B}\right) \equiv \vec{B} \circ \left(\nabla \times \vec{E}\right) - \vec{E} \circ \left(\nabla \times \vec{B}\right)$. For magnetospheric–ionospheric applications, the magnetic field energy density, to a very good approximation, greatly exceeds the electric field energy density. Poynting's theorem, given by (1), can then be written as

$$\iiint_V \frac{\partial}{\partial t}\left(\frac{B^2}{2\mu_0}\right) dV + \iiint_V \frac{\nabla \circ \left(\vec{E} \times \delta\vec{B}\right)}{\mu_0} dV + \iiint_V \vec{j} \circ \vec{E}\, dV = 0 \quad , \tag{2}$$

with $\delta\vec{B}$ representing the perturbation magnetic field due to the large-scale ionospheric current system (see Kelley et al. [1991]).

Poynting's theorem has been used to provide a general description of the energy exchange between the solar wind and magnetosphere [e.g., Hill, 1983; Cowley, 1991], for the interpretation of time-varying electromagnetic fields [e.g., Fraser, 1985], and, more recently, for the evaluation and interpretation of large-scale energy transfer in the ionosphere [e.g., Cowley, 1991; Kelley et al., 1991; Thayer and Vickrey, 1992; Gary et al., 1994]. For investigations concerned with high-latitude ionospheric energetics, the electromagnetic energy flux described by Poynting's theorem is a fundamental quantity because it describes the energy exchange between the magnetosphere and ionosphere. Joule heating and the bulk motion of the neutral gas in the high-latitude ionosphere are a direct result of this energy exchange. It is this more recent use of Poynting's theorem that will be developed further in our modeling study.

As stated by Cowley [1991], Poynting's theorem in the steady state demonstrates that any increase in plasma energy that occurs in one region of space must be at the direct expense of plasma energy that is lost in another, where the two regions are connected by a current tube. Thus, source regions where energy is transferred from the plasma to the electromagnetic field ($\bar{J} \circ \bar{E}$ negative) must be balanced by sink regions of energy transfer from the electromagnetic field to the plasma ($\bar{J} \circ \bar{E}$ positive). Based on this premise and the magnetic coupling of the magnetosphere and ionosphere at high latitudes, source or sink regions of electromagnetic energy flux in the high-latitude ionosphere must be matched by sink or source regions in the magnetosphere.

Frequently, the ionosphere is treated purely as a resistive load acting as a sink of electromagnetic energy being converted to thermal energy of the gas. This view, however, neglects the reactive nature of the high-latitude ionosphere due to the presence of neutral winds and their potential contribution to the electrodynamics. The neutral wind acts as a modifying influence in determining how much Poynting flux is required by the magnetosphere to power the dissipation processes in the high-latitude ionosphere and may potentially make the ionosphere a source of electromagnetic energy [Thayer and Vickrey, 1992]. Recently, Kelley et al. [1991] and

Gary et al. [1994] have shown through low-altitude, polar-orbiting satellite observations that the large-scale transfer of energy and momentum via the electromagnetic field between the solar wind-magnetosphere and the ionosphere-thermosphere at high latitudes can be determined by evaluating the DC component of the field-aligned Poynting flux. The derived results, interpreted from observations, have shown regions of electromagnetic energy flux into the ionosphere depicting the magnetospheric dynamo as an electrical source. However, electromagnetic energy flux out of the ionosphere over large scales has also been observed (see Gary et al. [1994]). The outward directed energy flux can be interpreted as having a generator in the ionosphere, presumably through the neutral wind dynamo mechanism.

Thayer and Vickrey [1992] investigated the neutral wind contribution to the high-latitude energetics by comparing two uncoupled systems — a magnetospheric circuit and an ionospheric circuit. They quantified the electrical energy contained in each system, separately, and demonstrated the importance of the neutral wind dynamo as a potential source of electrical energy at high latitudes. In that study, Thayer and Vickrey [1992] demonstrated the influence of the neutral wind on the Poynting flux by writing the steady-state form of Poynting's theorem as

$$-\iiint_V \frac{\nabla \circ \left(\vec{E} \times \delta\vec{B}\right)}{\mu_0}\, dV = \iiint_V \vec{j} \circ \vec{E}\; dV = \iiint_V \left\{\vec{j} \circ \vec{E}' + \vec{u}_n \circ \left(\vec{j} \times \vec{B}_0\right)\right\} dV \quad , \tag{3}$$

where $\vec{E}'$ is the electric field in the frame of reference of the neutral gas and $\vec{E}$ is the electric field in the inertial frame. From (3), the divergence of Poynting flux is equal to the volume energy transfer rate which is equal to the sum of the Joule heating rate and the mechanical energy transfer rate. As a positive definite quantity, the Joule heating rate is a sink of electromagnetic energy flux in the ionosphere, while the mechanical energy transfer rate could be a sink or source depending on the specific relationships among the neutral wind, conductivity, and electric field. By applying Gauss' theorem and following the arguments presented by Kelley et al. [1991], the divergence in the Poynting flux may be related to the vertical, or field-aligned, Poynting flux.

Equation 3 has important implications for studies of ionospheric and thermospheric energetics that involve a complex coupling amongst the conductivity, electric field and neutral wind. The determination of the electromagnetic energy flux is further complicated by the different response times of each of these parameters to changes in the M-I system. The response time for conductivity and neutral wind is also altitude dependent with, for example, the neutral wind responding more rapidly in the F region than in the E region to changes in the electric field. Therefore, determination of the field-aligned Poynting flux from measurement must insure that a quasi steady-state condition is reached in order to interpret those results using the source-sink concept. However, the different response times, specifically the long response of the neutral wind compared to changes in the electric field and conductivity, allow for the neutral wind affects on the M-I system to be investigated. This was first demonstrated by Lyons et al. [1985] by evaluating the polar cap currents resulting from "spun-up" neutral winds and setting the ion convection to zero. Deng et al. [1993] investigated the effects of the time-dependent neutral wind dynamo on the high-latitude ionospheric electrodynamics after a geomagnetic storm using the NCAR-TIGCM and found that the neutral wind contributes significantly to the ionospheric current system after the storm. They also calculated the electromagnetic energy flux but, unfortunately, used the independent generator calculations presented by Thayer and Vickrey [1992] and not the coupled expression. More recently, Lu et al. [1995] has used the AMIE technique to simulate substorm and equinox conditions and evaluate the high-latitude electromagnetic energy flux using the coupled expression described by Thayer and Vickrey [1992].

It is important to make the distinction between the divergence in the Poynting flux and the Joule heating rate of the gas. If the ionospheric current density and electric field are measured in the inertial reference frame, then the flux of electromagnetic energy describing the heat and momentum transfer of energy between the magnetosphere and ionosphere can be determined (as demonstrated by Kelley at al, 1991 and Gary et al., 1994). It is extremely important to note that an evaluation of the volume Joule heating rate requires a measure of the electric field in a

reference frame moving with the neutral gas at all altitudes. This electric field is not a quantity that is directly measured. The common practice of computing $\Sigma_p E^2$, where $\vec{E}$ is the electric field in the inertial frame and Σ_p is the height-integrated Pedersen conductivity, is not neccessarily a measure of the Joule heating rate. We point out here that substantial errors in both the magnitude of the Joule heating rate and in the momentum transfer rate to the neutral atmosphere may arise by making this assumption. However, the presence of the neutral wind is implicitly included in a measure of the field-aligned Poynting flux. Therefore, it is important to investigate the exchange of electromagnetic energy in the high-latitude ionosphere using this source–sink concept of Poynting's theorem to provide further insight into the M–I electrodynamic system. Here, we will pursue a modeling effort to treat the coupled aspects of the M–I system by evaluating the exchange of electromagnetic energy in the high-latitude ionosphere. As part of this effort, we demonstrate the important electrodynamic role of the neutral wind and its conductivity-weighted distribution in altitude. We also develop further the relationship of Poynting's theorem to ionospheric studies of Joule heating and neutral wind dynamics to elucidate the sources and sinks of electromagnetic energy in the high-latitude ionosphere.

2 APPROACH

Adopting the source-sink concept, we apply Poynting's theorem to the high-latitude ionosphere where the ionosphere is directly coupled to the magnetosphere through highly conducting magnetic field lines. Electromagnetic energy flux is transferred between the source and sink regions of the magnetosphere and ionosphere via electric fields and field-aligned currents. To study the sources and sinks of electromagnetic energy in the high-latitude ionosphere under steady-state conditions, we use the expression for Poynting's theorem described in (3). To model this expression we use the Vector Spherical Harmonic (VSH) model of Killeen et al. [1987] to provide the necessary thermospheric and ionospheric parameters.

The VSH model is based on a spectral representation of the output fields from the NCAR Thermosphere/Ionosphere General Circulation Model (TIGCM) simulations. The NCAR-TIGCM is a time-dependent, three-dimensional model that solves the fully coupled, nonlinear, hydrodynamic, thermodynamic, and continuity equations of the neutral gas self-consistently with the ion energy, ion momentum, and ion continuity equations (see Roble et al. [1988] and references therein). A simulation is uniquely determined by the input parameters to the model (i.e., EUV and UV fluxes, auroral particle precipitation, high-latitude ionospheric convection, and lower thermospheric tides). During a model run, the particle fluxes and the cross polar cap potential may be specified to remain fixed throughout the 24-hour model simulation. This type of model simulation is referred to as a diurnally reproducible state, meaning the model parameters are reproducible over a model day, and the "UT effects" associated with the diurnal migration of the geomagnetic pole about the geographic pole are incorporated. Although the diurnally reproducible state may not actually occur in nature, due to shorter term variations in the solar wind/magnetosphere interaction, the model simulation does provide a description of the global, UT-varying thermosphere-ionosphere system during a particular geophysical situation. A

set of NCAR-TIGCM runs have been expanded into VSH model coefficients that can be used to represent a range of geophysical conditions.

In the TIGCM formulation, the magnetosphere is treated as a generator delivering a fixed voltage to the ionosphere using the Heelis ion convection model [Heelis et al., 1982]. The parameterization of the ion convection pattern is tied to estimates of the total auroral hemispheric power input from the NOAA/TIROS particle flux measurements (H_p index). For the model simulation, any charge separation in the ionosphere due to neutral winds or gradients in conductivity are closed through field-aligned currents. Thus, for calculations of the electromagnetic energy flux, the neutral winds contribute to the current system while the electric field originates in the magnetosphere. The model ionosphere is coupled to the magnetosphere through the imposed electric field and particle precipitation, but no direct magnetospheric feedback is incorporated into the model to address how the processes in the ionosphere influence the magnetospheric response.

In this study, a model simulation providing a self-consistent description of thermosphere-ionosphere processes is used to study the coupled aspects of the M-I system at high latitudes. This approach differs from that used by Thayer and Vickrey [1992] in which the electrodynamic properties of the ionosphere and magnetosphere were evaluated separately to demonstrate the potential role the neutral winds could play in high-latitude electrodynamics. To make our calculations, we define a volume that covers the area from the geomagnetic pole to the 60°N magnetic latitude circle and extends in altitude from 110 to 400 km. We assume that the vertical magnetic flux tubes permeate this volume, each enclosing a 5°× 5° latitude / longitude bin. The calculations are performed at each grid point assuming horizontal uniformity of the parameters within each 5° bin. Applying these approximations to (3), the expression evaluated at each grid point in the modeling effort becomes

$$S_z = \int_z \vec{j} \circ \vec{E}\, dz = \int_z \left\{ \vec{j} \circ \vec{E}' + \vec{u}_n \circ \left(\vec{j} \times \vec{B}_0 \right) \right\} dz \quad , \tag{7}$$

where S_z is the field-aligned Poynting flux. The coordinate system employed is right-handed with $\hat{x}$ directed positive northward, $\hat{y}$ directed positive eastward, and $\hat{z}$ directed positive downward.

The model simulation used extensively in this study is representative of moderate to quiet geomagnetic activity (H_p index = 11 GW and cross-cap potential = 60 kV) and solar maximum conditions ($F_{10.7} = 220 \times 10^{-22}$ W m^{-2} sec^{-1}). Polar plots (from the model simulation for the December solstice in the northern hemisphere at 4 UT) of the electric field magnitude in mV/m and the height-integrated Pedersen conductivity in mhos are shown in Figure 1a and b, respectively, on a magnetic latitude/magnetic local time grid extending in magnetic latitude from 60°N to the geomagnetic pole. The electric field magnitude shown in Figure 1 represents a two-cell ion convection pattern with its greatest values found inside the polar cap. The strong electric field over the polar cap will be used to demonstrate that significant ion-neutral coupling results in a small downward electromagnetic energy flux that would otherwise be large if the neutral winds were neglected. Thus, the electric field contribution to the net electromagnetic energy flux is compensated by the electric field's influence on driving the neutral wind. Evidence of this effect will be demonstrated in the following sections. The distribution of the height-integrated Pedersen conductivity is structured across the polar cap with enhanced values in the midnight and dawn sectors and a factor of three reduction in magnitude inside the polar cap. The enhanced regions of conductivity are due to the NCAR-TIGCM formulation for auroral particle precipitation (Roble and Ridley, 1987).

Figure 1c and d is an altitude plot of the local Pedersen and Hall conductivity in mhos/m along the dawn-dusk magnetic meridian. The local Pedersen conductivity peaks near 130 km with enhancements in the dawn and dusk sectors of the E region and moderate conductivity

values in the polar cap in both E and F regions. The local Hall conductivity is limited to the E region with peak values near 115 km and an asymmetric distribution across the polar cap with maxima found in the dawn sector. These parameters are important contributors to the net electromagnetic energy flux into the ionosphere and will be used in the evaluation of (7). The neutral wind contribution to (7) will be discussed in more detail in the following section. Due to the coarse $5° \times 5°$ grid of the NCAR-TIGCM, the model parameterizations, and the inherent smoothing of the spectral representation by the VSH model, the model output variables represent only the large-scale features of the system, as discussed by Deng et al. (1993).

3 ANALYSIS

We begin the analysis by evaluating the height-integrated energy transfer rate, $\vec{J} \circ \vec{E}$, in the high-latitude ionosphere which, from (7), is equal to the field-aligned Poynting flux. The relationship of the energy transfer rate, or the electromagnetic energy flux, to the electric field, conductivity, and neutral wind can be shown by expanding (7) to give the expression

$$\int_z \vec{j} \circ \vec{E}\, dz = \Sigma_p E^2 + \vec{E} \circ \int_z \sigma_p \left(\vec{u}_n \times \vec{B}\right) dz + \vec{E} \circ \int_z \sigma_h \vec{u}_n \left|\vec{B}\right| dz \quad , \tag{8}$$

where σ_p and σ_h are the local Pedersen and Hall conductivities and Σ_p is the height-integrated Pedersen conductivity. The total electromagnetic energy flux calculated from (8) for the model run described in the approach section is displayed in Figure 2a on a magnetic latitude/magnetic local time grid in units of milliWatts per square meter for the northern winter hemisphere at 4 UT. The distribution of electromagnetic energy flux shown in Figure 2a is representative of the field-aligned Poynting flux at high latitudes. The electromagnetic energy flux is predominantly directed into the entire polar ionosphere with dawn sector values between 2.0 and 3 .0 mW/m^2, polar cap values less than 1.0 mW/m^2, and dusk sector values between 1.0 and 1.5 mW/m^2. An asymmetry in the electromagnetic energy flux across the noon-midnight meridian is apparent in Figure 2a with more electromagnetic energy flux directed into the ionosphere in the morning sector (00 - 12 MLT) than in the evening sector (12 - 00 MLT) by a factor of two or more. Weak regions of negative electrical energy flux or upward Poynting flux (less than -0.1 mW/m^2) are determined from the model and are located in the regions near the ion convection reversals. These features of negative electrical energy flux are caused by the electrical contribution of the neutral wind as will be discussed in the following section. If the electromagnetic energy flux in

Figure 2a is integrated over the area of the polar cap, 90° to 60° magnetic latitude, the total electromagnetic power into the ionosphere is approximately 3.5×10^{11}W.

Figure 2b illustrates the total electromagnetic energy flux from a more geomagnetically active simulation using a cross-cap potential of 90 kV and an H_p Index of 33 GW. The active case has features very similar to those discussed for the less active case shown in Figure 2a, however the magnitude of the electromagnetic energy flux in the auroral zone has increased proportionally by a factor of about 3. The polar cap values in Figure 2b are of similar magnitude to those of the less active case.

Recently, Gary et al. [1995] provided statistical averages of the field-aligned DC Poynting flux determined from DE 2 throughout the polar cap. Using DE-2 data of ion drift velocities and magnetic fields, the field-aligned Poynting flux was calculated for some 576 orbits over the satellite lifetime using the technique described by Gary et al. [1994]. The data were sorted for interplanetary magnetic field conditions (northward and southward IMF) and geomagnetic activity ($K_p \leq 3$ and $K_p > 3$) and binned by invariant latitude and magnetic local time. In general, it was found that the average field-aligned Poynting flux is directed into the ionosphere throughout the entire polar cap, as was determined from the model simulation. The magnitudes of the averaged Poynting flux are reasonably reproduced by the model results shown in Figure 2a,b. Asymmetries in the average Poynting flux for both high and low K_p were determined from the observations with the dawn and noon sectors having greater values than in the dusk and midnight sectors. The observed asymmetry between the dawn and dusk sectors corresponds well with that determined from the model. However, the model also predicts a strong region of downward Poynting flux in the midnight sector that is not observed in the data. This may be due to the parameterization of the particle precipitation used in the model and to the averaging over all seasons of the DE-2 data.

When averaging the DE-2 data during conditions of only upward Poynting flux it was found that the magnitudes never exceeded -2.25 mW/m^2 anywhere within the polar cap. An interesting feature in the DE-2 data set is the significant occurrence and magnitude of upward Poynting flux in the predawn sector during periods of southward IMF and high K_p conditions. The results of the coupled model shown in Fig 2a,b illustrate much weaker regions of upward Poynting flux near the convection reversal locations.

Term Analysis

The distribution of each of the height-integrated terms given in (8) along the dawn-dusk magnetic plane in units of milliWatts per square meter is illustrated in Figure 3 to demonstrate their relative contributions to the total electromagnetic energy flux shown in Figure 2a. The total electromagnetic energy flux is given by the solid line in Figure 3 and shows the asymmetric distribution of energy flux between the dawn and dusk sectors. The first term on the RHS of (8), Term 1, is a positive definite quantity accounting for the resistive dissipation of electromagnetic energy and, as shown by the dashed line in Figure 3, is the dominate term contributing to the positive or downward flux of electromagnetic energy into the ionosphere. Term 1 peak values of 2.0 mW/m^2 occur in the polar cap with nearly equal enhancements of 1.5 mW/m^2 located in the dawn and dusk sectors. The other two terms in (8) account for the electric field–neutral wind coupling in the ionosphere and tend to reduce the net flux of electromagnetic energy directed into the ionosphere. Term 2, the Pedersen term, is the main contributor to the reduction in the downward energy flux, as shown by the dotted line in Figure 3, with peak values in the polar cap of –1.7 mW/m^2 and values of –0.7 mW/m^2 and –0.3 mW/m^2 in the dusk and dawn sectors, respectively. Strong ionospheric coupling between the neutral wind and the electric field in the dusk and polar cap regions and weak coupling in the dawn sector accounts for the asymmetry in the dawn-dusk distribution of Term 2 and is responsible for the asymmetry in the dawn-dusk distribution of the total electromagnetic energy flux. Term 3, the Hall term, is small everywhere with values in the dawn sector of about 0.2 mW/m^2 and –0.1 mW/m^2 in the polar cap.

To illustrate the height dependencies in evaluating the integrals in (8), model calculations are made for each term along the dawn-dusk plane at 5 km increments from 110 to 400 km. Figure 4 is a plot of the altitude distribution for each term integrated in (8) and displayed in Figure 3. Figure 4a represents the distribution in altitude of Term 1 along the dawn-dusk plane in units of 1.0×10^{-7} mW/m^3. The main contribution to this positive definite term comes from the E region with enhancements in the dawn, dusk, and polar cap regions. The enhancement in the polar cap is due to the presence of strong electric fields in this region, while enhancements in the dawn and dusk sector are due primarily to enhancements in the conductivity (with greater Pedersen conductivity in the dawn sector than in the dusk sector). Lesser contributions made at altitudes above the E region are also limited to dawn, dusk, and polar cap regions. A noticeable contribution to Term 1 from the F region can be seen in the polar cap where soft particle precipitation enhances the Pedersen conductivity (see Figure 1c).

The altitude distribution of Term 2 is illustrated in Figure 4b. This term accounts for the coupling between the electric field and the Pedersen-weighted neutral wind. Throughout all altitudes this term is predominantly negative, with most of the contribution coming from altitudes above 140 km. As illustrated by the integrated result for Term 2 in Figure 3, the main contributions come from the dawn, dusk, and polar cap regions with contributions from F region and E region altitudes. The greatest contribution to Term 2 comes from the polar cap at F-region altitudes, where the neutral winds are strongly coupled to the electric field. The magnitude of Term 2 with increasing altitude is quite uniform in both the dawn and dusk sectors as a reduction in Pedersen conductivity is countered by an increase in the neutral wind. The dawn and dusk sectors illustrate the asymmetric pattern seen in the integrated result throughout all altitudes. The altitude invariance of this term demonstrates that the F-region ion convection is strongly imposed on the neutral circulation well into the E region. This is a very important aspect of the model simulation as this term is the dominant one in reducing the total electromagnetic energy flux into the ionosphere.

The coupling between the electric field and Hall-weighted neutral wind, Term 3, is displayed in Figure 4c showing its altitude distribution to be isolated to the lower E region and concentrated in the dawn and polar cap sectors. The height distribution is limited by the Hall conductivity, as was shown in Figure 1d, while the distribution along the dawn-dusk plane is attributable to the relationship between the electric field and the neutral wind. The neutral winds in the lower E region are a factor of three to four less in magnitude than winds in the F region. The lower E region neutral wind pattern is also rotated counter clockwise compared to the F region circulation and favors a more cyclonic neutral wind circulation. These variations in the neutral wind with height are a result of the complex interaction between tidal forcing and magnetospheric forcing in the E region as is discussed by Mikkelsen and Larsen [1991]. Because of the counter clockwise rotation of the wind pattern with decreasing altitude, the winds in the polar cap are in opposite direction to the imposed dawn-dusk electric field, resulting in a negative energy flux. However, due to the more cyclonic behavior of the E-region winds, the electric field and winds in the dawn sector are in the same direction, resulting in a positive energy flux. Because this term does not contribute to the Joule heating rate, a positive energy flux is representative of electrical energy being converted to mechanical energy, while a negative energy flux is representative of mechanical energy converted to electrical energy. This term is less important after height integration, yet, it represents a contribution that is typically not accounted for in studies of electrodynamics at high latitudes.

The altitude distribution of the net electromagnetic energy flux per meter along the dawn-dusk plane is displayed in Figure 4d. The greatest contribution to the electrical energy flux comes from the E region where Term 1 dominates. The dawn-dusk distribution of positive electromagnetic energy flux per meter in the E region is skewed toward the dawn sector as Term 3 and Term 1 contribute positively in this sector. In the E-region dusk sector, positive electromagnetic energy flux per meter is reduced due to Term 2. In the F region, the electromagnetic energy flux per meter is negative due to the dominating negative contribution from Term 2. As will be shown, a net electromagnetic energy flux is indicative of the condition

where the component of the conductivity-weighted neutral wind in the $\vec{E} \times \vec{B}$ direction exceeds the $\vec{E} \times \vec{B}$ plasma drift velocity.

4 DISCUSSION

In the previous section we demonstrated that the neutral wind coupled with the electric field contributes significantly to reducing the DC field-aligned Poynting flux into the ionosphere, particularly in the polar cap and dusk sector. If it is assumed that the magnetic field is independent of height over our altitude range, an effective neutral wind can be determined to describe the height-integrated neutral wind profile weighted by the conductivity.

$$\vec{U}_{eff} = \frac{\int_z \sigma_p \vec{u}_n \, dz + \int_z \sigma_h \hat{b} \times \vec{u}_n \, dz}{\Sigma_p} \quad . \tag{9}$$

The effective neutral wind from (9) for the model simulation used above is displayed in Figure 5 with the same format as Figure 2. The resultant effective neutral wind has a pattern similar to that of the F region (see Thayer and Killeen [1993]) with speeds reduced by approximately 50%. There is also a small counter clockwise twist of the pattern due to the contribution from E region altitudes (see discussion by Mikkelsen and Larsen [1991]). The weighting of the neutral wind with height by the ionospheric conductivity results in a combined influence of neutral wind dynamics and conductivity variations with altitude.

Using (9), the electromagnetic energy flux may be written in a more informative way as

$$\int_z \vec{j} \circ \vec{E} \, dz = \Sigma_p \left[E^2 - \vec{U}_{eff} \circ \left(\vec{E} \times \vec{B} \right) \right] \quad . \tag{10}$$

Expressed in this form, the effective neutral wind acts as a modifying influence on what fraction of Poynting flux energy supplied by the magnetosphere is involved in dissipation processes in the high-latitude ionosphere, as discussed previously. However, the neutral wind's influence

may make the ionosphere a source of electromagnetic energy ($\vec{J} \circ \vec{E}$ negative) if the effective neutral wind has a component in the $\vec{E} \times \vec{B}$ direction that exceeds the $\vec{E} \times \vec{B}$ plasma drift velocity. The negative or upward Poynting flux regions discussed above are located near the convection reversal boundaries where the effective neutral wind in the $\vec{E} \times \vec{B}$ direction exceeds the plasma drift velocity. At the convection reversal boundaries there is no Poynting flux, because the electric field is zero. In the polar cap, small or near-zero downward Poynting flux can also occur as the effective neutral wind is antisunward and approaches the velocity of the $\vec{E} \times \vec{B}$ plasma drift due to complementary pressure gradient and ion drag forces. Individual DE-2 orbits of the Poynting flux from Gary et al. [1994] have shown small and near-zero values for the downward Poynting flux inside the polar cap.

Thus, it is the component of the effective neutral wind in the $\vec{E} \times \vec{B}$ direction that is important for energetics in the steady state, not the effective neutral wind vector itself. Because the effective neutral wind is very similar to the $\vec{E} \times \vec{B}$ plasma drift in the dusk and polar cap regions, an asymmetry in the high-latitude distribution of the electromagnetic energy flux results. The influence of the effective neutral wind coupled to the electric field is illustrated in Figure 3 by combining the results of Term 2 and Term 3 from (8). Referring to Figure 3, the enhancement of negative energy flux in the polar cap is a result of the effective neutral wind having a strong component in the $\vec{E} \times \vec{B}$ direction. The asymmetry in the negative electromagnetic energy flux from Term 2 and 3 between the dawn and dusk sectors reflects the dawn-dusk asymmetry demonstrated by the effective neutral wind pattern shown in Figure 5. This asymmetry has also been observed in the F region neutral circulation pattern [e.g., Thayer and Killeen [1993]. Thayer and Killeen [1993] demonstrated that an ion convection pattern with dawn and dusk cells of equal and opposite potential results in an asymmetric neutral circulation pattern with the dawn cell less organized than the dusk cell. Gundlach et al. [1988] explain this asymmetry in terms of the disparate balance of hydrodynamic forces between the dusk and dawn sectors. In Figure 3, the higher positive values of the net electrical energy flux (solid line) in the dawn sector demonstrate that the effective neutral wind is less coupled to the electric field in the dawn sector

than in the dusk sector. Overall, the neutral wind contribution to the energy flux in the ionosphere is significant, particularly in the polar cap and dusk sector (as was concluded by Thayer and Vickrey [1992]).

We have shown that the neutral wind contributes significantly to the overall electromagnetic energy flux in the high-latitude ionosphere. However, we have not determined how much the neutral wind is contributing to the Joule heating of the gas or to the mechanical energy of the gas. The partitioning of electromagnetic energy flux into its sinks (kinetic and internal energy of the gas) and sources (electrical energy caused by the neutral wind dynamo) can be addressed by evaluating separately the Joule heating rate and mechanical energy transfer rate described in (3).

Joule Heating Rate

The Joule heating rate is a positive definite quantity acting purely as a sink of electromagnetic energy in the ionosphere as electrical energy is transferred to the internal energy of the gas as heat. The height-integrated Joule heating rate can be obtained without approximation given the height distribution of the neutral wind, electric field, and conductivity as described by the expression

$$\int_z \vec{j} \circ \vec{E}' \, dz = \int_z \vec{j} \circ \left(\vec{E} + \vec{u}_n \times \vec{B}\right) dz = \int_z \sigma_p \left(\vec{E} + \vec{u}_n \times \vec{B}\right)^2 dz \quad . \qquad 11)$$

An illustration of the height-integrated Joule heating rate for the simulation described in the previous sections is given in Figure 6. The main features of the Joule heating pattern are enhanced regions of Joule heating in the auroral oval with maxima in the dawn and post-midnight sectors and relatively weak enhancements in the dusk sector and inside the polar cap. The Joule heating rate displays an asymmetric pattern in the auroral zone with the Joule heating rate in the dawn sector a factor of three greater than in the dusk sector. Comparing these results with the electromagnetic energy flux calculations given in Figure 2, we find that the magnitude and pattern of the Joule heating rate is very similar to the electromagnetic energy flux. Thus, most of the electromagnetic energy flux directed into the ionosphere is dissipated as heat under the conditions of this simulation. That is not to say that the neutral winds contribute insignificantly to the distribution of the electromagnetic energy flux at high latitudes, but that the winds are contributing most to the Joule heating rate of the gas.

To elucidate the impact of the neutral wind on the Joule heating rate at high latitudes, a calculation of the Joule heating rate neglecting the neutral wind is shown in Figure 6b. Neglecting the neutral wind has its greatest impact in the dusk sector and central polar cap where the Joule heating rate is overestimated by as much as a factor of three. This makes the point that, although the electric field or conductivity may be enhanced in these regions, the neutral winds

are also strongly coupled to the electric field resulting in a much lower Joule heating rate than might be anticipated if the winds are ignored.

Because the Poynting flux approach implicitly accounts for the neutral wind and describes the net electromagnetic energy flux between the magnetosphere and ionosphere, it is a fundamental measure of energy transfer in the system. As we have just shown, the Joule heating rate is a significant part of the electromagnetic energy flux. Given a better understanding for the quantities $\vec{j} \circ \vec{E}$ (the electromagnetic energy flux) and $\vec{j} \circ \vec{E}'$ (the Joule heating rate), it is worth reviewing the approaches taken by many investigators in evaluating, empirically, the Joule heating rate in the high-latitude ionosphere and how these approaches relate to the electromagnetic energy flux. These investigations are mainly to quantify the height-integrated Joule heating rate to describe the change in the internal energy of the gas caused by the dissipation of electrical energy in the ionosphere. Because of the difficulty in determining the neutral wind with height, approximations to the neutral wind are typically made when calculating the Joule heating rate from measurements. However, the manner in which the approximation to the neutral wind is treated can result in different interpretations for the evaluated Joule heating rate and subsequently the electromagnetic energy flux.

For the case when the height distribution of the conductivity and electric field (typically assumed independent of height) are known and the neutral wind is assumed to be zero, the form of the height-integrated Joule heating rate is $\vec{J} \circ \vec{E}' = \vec{J} \circ \vec{E} = \Sigma_p E^2$. This form of the equation represents the electromagnetic energy flux and means that the mechanical energy of the gas is zero. Thus, electromagnetic energy from the magnetosphere described by the divergence in the Poynting flux is dissipated entirely in the ionosphere (acting purely as a resistive load described by the height-integrated Pedersen conductivity) as thermal energy. This can be considered the standard approach used in many investigations of high-latitude energetics [e.g., Banks et al., 1981; Foster et al., 1983]. We have demonstrated in Figure 6 that this assumption can be quite misleading, particularly in the dusk sector and the central polar cap.

A different interpretation results for this case if the height distribution of the current density instead of the conductivity, is known. For instance, if the current distribution is determined by solving the expression $\vec{j} = en_e\left(\vec{V}_i - \vec{V}_e\right)$ from measurements at different altitudes, say from radar measurements (e.g., Kamide and Brekke [1993]), and the neutral wind is assumed zero, then the height-integrated Joule heating rate is actually the total electromagnetic energy flux converted, dissipated, or generated in the ionosphere. This can be seen more clearly by expressing the current density in the form $\vec{j} = \vec{\sigma} \circ \left(\vec{E} + \vec{u}_n \times \vec{B}\right)$. This shows that the height distribution of the neutral wind is implicit within the measurement of $\vec{j}$. Also, the Joule heating rate is a positive definite quantity, but the determination of $\vec{j} \circ \vec{E}$ could be of either sign, as discussed by Thayer and Vickrey [1992]. The same result occurs if the height-integrated current density and the electric field are determined from a satellite measurement of $\vec{E}$ and $\delta\vec{B}$, exemplified by the recent DE-2 field-aligned Poynting flux results described by Gary et al. [1994].

In more general terms, if the neutral wind is contributing at all to the energetics, it is implicitly contained within the current density and the electric field; the distribution between these two depends on the electrical coupling between the ionosphere and magnetosphere. Irrespective of whether neutral wind contributions are contained in the current density or electric field, their effects on the net electromagnetic energy flux are accounted for if both the current density and electric field are determined. Furthermore, the measure of the electromagnetic energy flux is a more fundamental quantity than the Joule heating rate and may be more accurately determined from spacecraft or ground-based radars capable of measuring the electric and magnetic field.

Mechanical Energy Transfer Rate

The mechanical energy transfer rate is either a sink or source of electromagnetic energy flux depending on whether electromagnetic energy is converted into the bulk motion of the gas (sink) or generated by the motion of the neutral gas through dynamo action (source). In this steady-state model simulation, the conductivity-weighted neutral wind acts as an electrical source

by contributing to the current distribution in the ionosphere. As a sink of electromagnetic energy, the conductivity-weighted neutral wind is powered by the $\vec{J} \times \vec{B}$ force. The sign of the mechanical energy transfer rate illustrates whether the neutral wind is opposite (negative) or in the direction of (positive) the $\vec{J} \times \vec{B}$ force. A negative mechanical energy transfer rate would indicate that the neutral winds are opposing the $\vec{J} \times \vec{B}$ force and energy is transformed from mechanical form to electrical form, and vice versa.

Figure 7 is a plot of the height-integrated mechanical energy transfer rate, Joule heating rate, and the total electromagnetic energy flux along the dawn-dusk plane, similar in format to Figure 3. The height-integrated Joule heating rate in Figure 7 (dashed line) accounts for much of the electromagnetic energy flux into the ionosphere (solid line), as was demonstrated by Figure 6. The mechanical energy transfer rate is positive in the dawn and dusk sectors and negative in the polar cap. The positive mechanical energy transfer rate in the dawn and dusk sectors, therefore, acts as a sink of electromagnetic energy. Here, electrical energy is being converted to the mechanical energy of the gas in an effort to maintain sunward plasma flow in these sectors. In the polar cap, the mechanical energy transfer rate acts as a source of electrical energy as the winds are complemented by pressure gradient and ion drag forces. Figure 8 is a plot of the percent contribution from the Joule heating rate (dashed line) and the mechanical energy transfer rate (dotted line) to the net electromagnetic energy flux. The percent relative contribution of the Joule heating rate and mechanical energy transfer rate is determined by the expression $\frac{|J|}{|J|+|M|} * 100.$ and $\frac{|M|}{|J|+|M|} * 100.$, respectively. In the dawn and dusk sectors, the contribution from the mechanical energy transfer rate varies between 10 and 30%. In the polar cap, where the mechanical energy transfer rate is negative, the contribution to the electromagnetic energy flux is also between about 10 and 30%. In the locations near the ion convection reversal boundaries, the mechanical energy transfer rate can contribute as much as the Joule heating rate, allowing for the possibility of a net upward Poynting flux.

weak contribution from the Hall term, and the always positive Joule heating rate precludes the existence of a large, sustained upward Poynting flux under these modeled conditions and quite possibly in nature, as demonstrated by the DE-2 results.

4 CONCLUSIONS

We investigated the exchange of electromagnetic energy in the high-latitude ionosphere using a steady-state, source-sink concept of Poynting's theorem to provide further insight into the M–I electrodynamic system. Poynting's theorem applied to the high-latitude M–I system and the theorem's relationship with the Joule heating rate and mechanical energy transfer rate has been elucidated and the consequences of this relationship evaluated through numerical modeling. Because the Poynting flux approach accounts for the neutral wind, implicitly, and describes the net electromagnetic energy flux between the magnetosphere and ionosphere, it represents a fundamental measure of energy transfer in the system. The Joule heating rate is a significant part of the energy exchange but requires accurate modeling of the neutral wind. Evaluation of the contributing factors to the electromagnetic energy flux has a strong dependence on the extent of the coupling among the conductivity, neutral wind, and electric field throughout the E and F regions.

Here, we used the VSH model to provide the necessary thermosphere–ionosphere parameters to evaluate and interpret the electromagnetic energy flux at high latitudes for moderate to quiet geomagnetic conditions during solar maximum. Although the model is coupled to the magnetosphere through the mapping of the magnetospheric electric field and particle precipitation, no direct feedback to the magnetosphere has been attempted. To this end, any neutral wind dynamo action in the model would be manifested in terms of currents, with the magnetosphere acting as a pure voltage generator. The analysis of the steady-state electromagnetic energy flux at high latitudes under the model conditions of moderate to quiet geomagnetic activity, December solstice, solar maximum has lead to a number of conclusions.

- The electromagnetic energy flux, or field-aligned Poynting flux, is predominantly directed into the high-latitude ionosphere with weak regions of upward electromagnetic energy flux near the boundaries of the convection reversals. The distribution of electromagnetic energy flux at high latitudes is asymmetric with greater downward flux in the morning sector than in the evening sector. The region of the polar cap has the lowest values of downward electromagnetic energy flux.

- The Joule heating rate accounts for much of the electromagnetic energy converted in the ionosphere with the conductivity-weighted neutral wind contributing significantly to the Joule heating rate and, thus, affecting the net electromagnetic energy flux between the magnetosphere and ionosphere.

- On average, the mechanical energy transfer rate amounts to about 10% to 30% of the net electromagnetic energy flux in the dawn, dusk, and polar cap regions, acting as a sink of electromagnetic energy flux in the dawn and dusk sectors and as a source of electromagnetic energy flux in the polar cap.

- Weak upward electromagnetic energy flux is found in the regions near the convection reversal boundaries due to the mechanical energy transfer rate exceeding the Joule heating rate. The upward electromagnetic energy flux was found to be small partly due to the relation of the conductivity-weighted neutral wind to the imposed electric field and partly due to the Joule heating rate increasing irrespective of the source of electromagnetic energy flux.

This analysis of the electromagnetic energy flux at high latitudes has led to a better understanding of the significance of Poynting flux measurements. Moreover, it tests the models in their ability to properly address the extent of the coupling among the conductivity, neutral wind, and electric field throughout the E and F regions. It is apparent from the simulations used in this study that the neutral wind is strongly coupled to the electric field well into the E region.

Observational evidence of the electrical coupling with altitude needs to be gathered to validate the model's electrical characteristics, particularly in the E region. An outstanding question that needs observational support is to what extent do the tidal forces from below and electric field forces from above influence the electrical coupling in the E region. Measurements in the central polar cap may be most effective in addressing this issue as the electric field, neutral wind, and conductivity can be significant in this region, but yet, the net electromagnetic energy flux is small.

Acknowledgments. This work was supported by NASA, Contract NAS5-31214, NASA Grant NAGW-3508. We would like to thank Dr. Tim Killeen, Rob Raskin, and Alan Burns at the University of Michigan for the VSH model code.

6 REFERENCES

Banks, P.M., J.C. Foster, and J.R. Doupnik, Chatanika radar observations relating to the latitudinal and local time variations of Joule heating, *J. Geophys. Res., 86*, 6869-6878, 1981.

Brekke, A., and C.L. Rino, High-resolution altitude profiles of the auroral zone energy dissipation due to ionospheric currents, *J. Geophys. Res., 83*, A6, 2517-2524, 1978.

Cowley, S.W.H., Acceleration and heating of space plasmas: basic concepts, *Ann. Geophys., 9*, 176-187, 1991.

Deng, W., T.L. Killeen, A.G. Burns, R.G Roble, J.A. Slavin, and L.E. Wharton, The effects of neutral inertia on ionospheric currents in the high-latitude thermosphere following a geomagnetic storm, *J. Geophys. Res., 98*, 7775-7790, 1993.

Foster, J.C., J.-P. St.-Maurice, and V.J. Abreu, Joule heating at high latitudes, *J. Geophys. Res., 88*, 4885-4896, 1983.

Fraser, B.J., Observations of Ion Cyclotron waves near synchronous orbit and on the ground, *Space Sci. Rev., 42*, 357-374, 1985.

Gary, J.B., R.A. Heelis, W.B. Hanson, and J.A. Slavin, Field-aligned poynting flux observations in the high-latitude ionosphere, *J. Geophys. Res., 99*, 11417-11427, 1994.

Gary, J.B., R.A. Heelis, J.P. Thayer, Summary of field-aligned poynting flux observations from DE-2, in press,*Geophys. Res. Lett*, 1995.

Gundlach, J.P., M.F. Larsen, and I.S. Mikkelsen, A simple model describing the nonlinear dynamics of the dusk/dawn asymmetry in the high-latitude thermospheric flow, *Geophys. Res. Lett., 15*, 307-310, 1988.

Heelis, R.A., J.K. Lowell, and R.W. Spiro, A model of the high-latitude ionospheric convection pattern, *J. Geophys. Res.*, 87, 6339-6345, 1982.

Heelis, R.A., and W.R. Coley, Global and local Joule heating effects seen by DE 2, *J. Geophys. Res., 93*, 7551-7557, 1988.

Hill, T.W., Solar-wind magnetosphere coupling, in *Solar-Terrestrial Physics*, pp. 261-302, R.L. Carovillano and J.M. Forbes, eds. (D. Reidel Publishing Company), 1983.

Kamide, Y., and A. Brekke, Altitude variations of ionospheric currents at auroral latitudes, *Geophys. Res. Lett., 20*, 309-312, 1993.

Kelley, M.C., D.J. Knudsen, and J.F. Vickrey, Poynting flux measurements on a satellite: a diagnostic tool for space research, *J. Geophys. Res., 96*, A1, 201-207, 1991.

Killeen, T.L., R.G. Roble, and N.W. Spencer, A computer model of global thermospheric winds and temperatures, *Adv. Space Res., 7*, 207-215, 1987.

Lu, G., A.D. Richmond, B.A. Emery, and R.G. Roble, Magnetosphere-ionosphere-thermosphere coupling: effect of neutral winds on energy transfer and field-aligned current, submitted to *J. Geophys. Res.*, 1995.

Lyons, L.R., T.L. Killeen, and R.L. Walterscheid, The neutral wind "flywheel" as a source of quiet-time, polar-cap currents, *Geophys. Res. Lett., 12*, 101-104, 1985.

Mikkelsen, I.S., and M.F. Larsen, A numerical modeling study of the interaction between the tides and the circulation forced by high-latitude plasma convection, *J. Geophys. Res., 96*, 1203-1213, 1991.

Roble, R. G. and E. C. Ridley, An auroral model for the NCAR thermospheric general circulation model, Annales Geophysicae, 5A, 369-382, 1987

Roble, R.G., E.C. Ridley, A.D. Richmond, and R.E. Dickinson, A coupled thermosphere/ ionosphere general circulation model, *Geophys. Res. Lett.*, *15*, 1325-1328, 1988.

Thayer, J.P., and J.F. Vickrey, On the contribution of the thermospheric neutral wind to high-latitude energetics, *Geophys. Res. Lett.*, *19*, 3, 265-268, 1992.

Thayer, J.P., and T.L. Killeen, A kinematic analysis of the high-latitude thermospheric neutral circulation pattern, *J. Geophys. Res.*, *98*, 11549-11565, 1993.

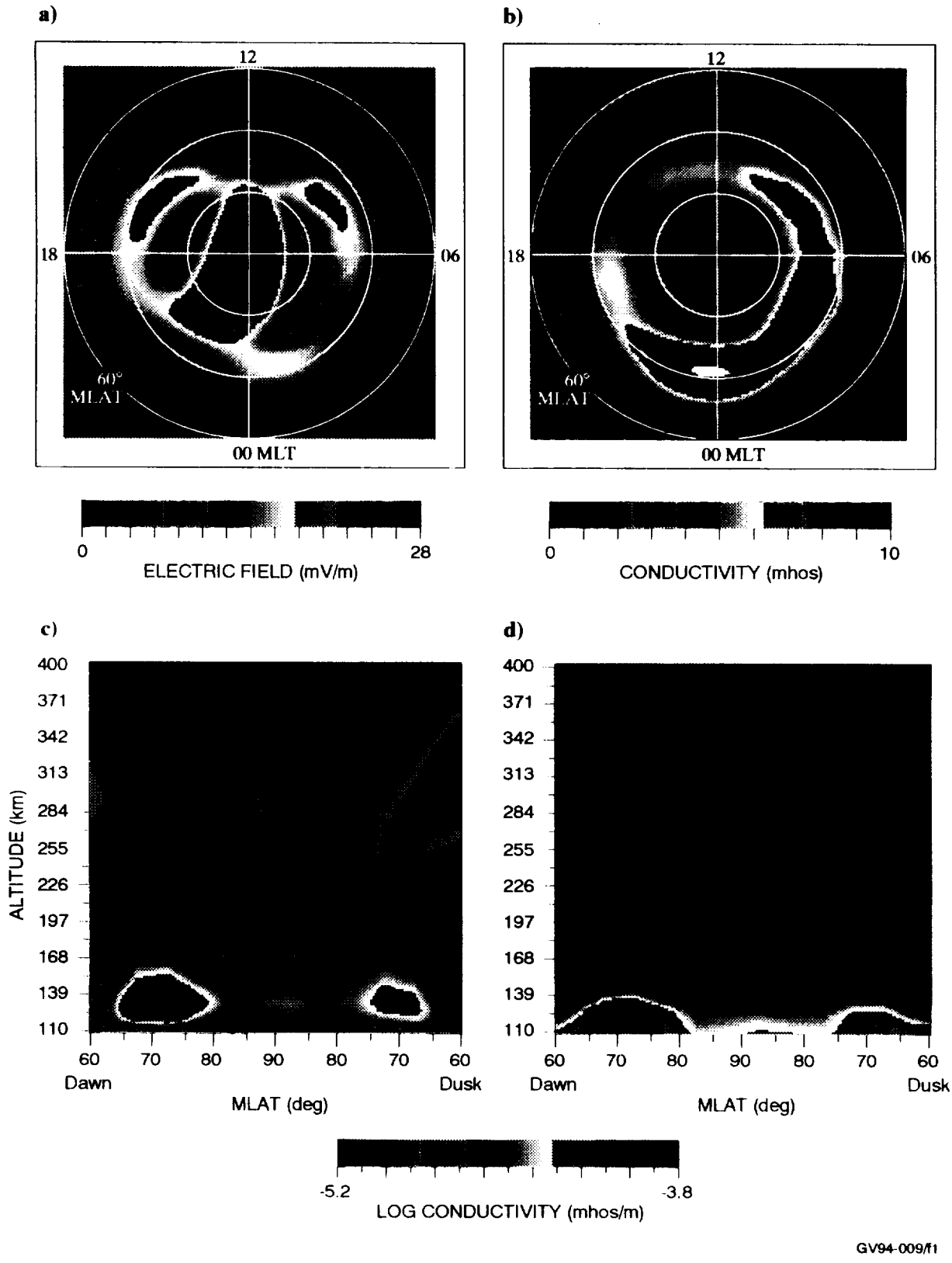

Fig. 1. Polar plots on a magnetic grid of a) electric field magnitude in mV/m b) height-integrated Pedersen conductivity in mhos. Altitude plots along the dawn-dusk magnetic plane of the local c) Log Pedersen and d) Log Hall conductivity in mhos/m.

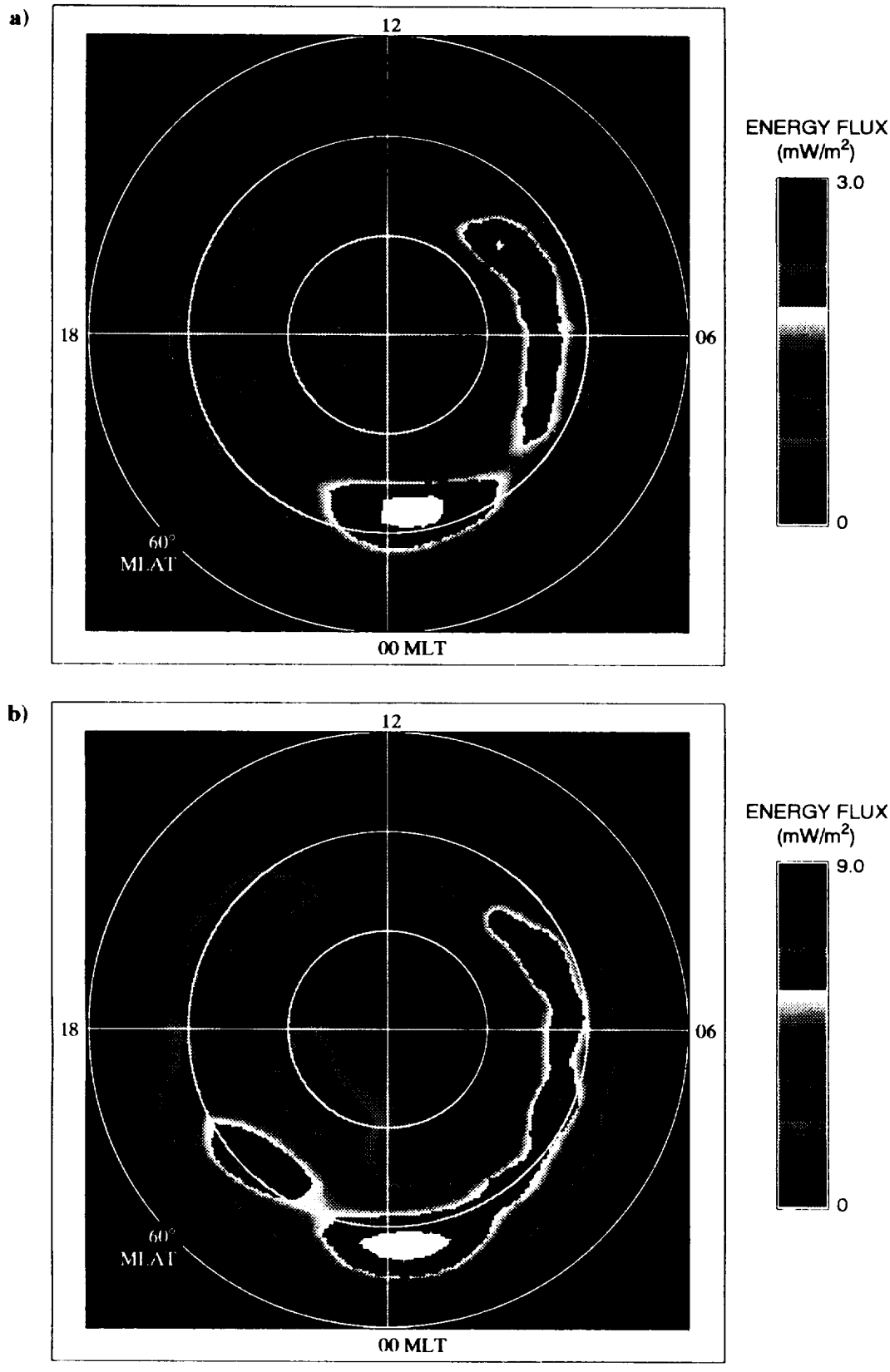

Fig. 2. Polar plots on a magnetic grid of the distribution of electromagnetic energy flux for a) 60 kV cross-cap potential and b) 90 kV cross-cap potential.

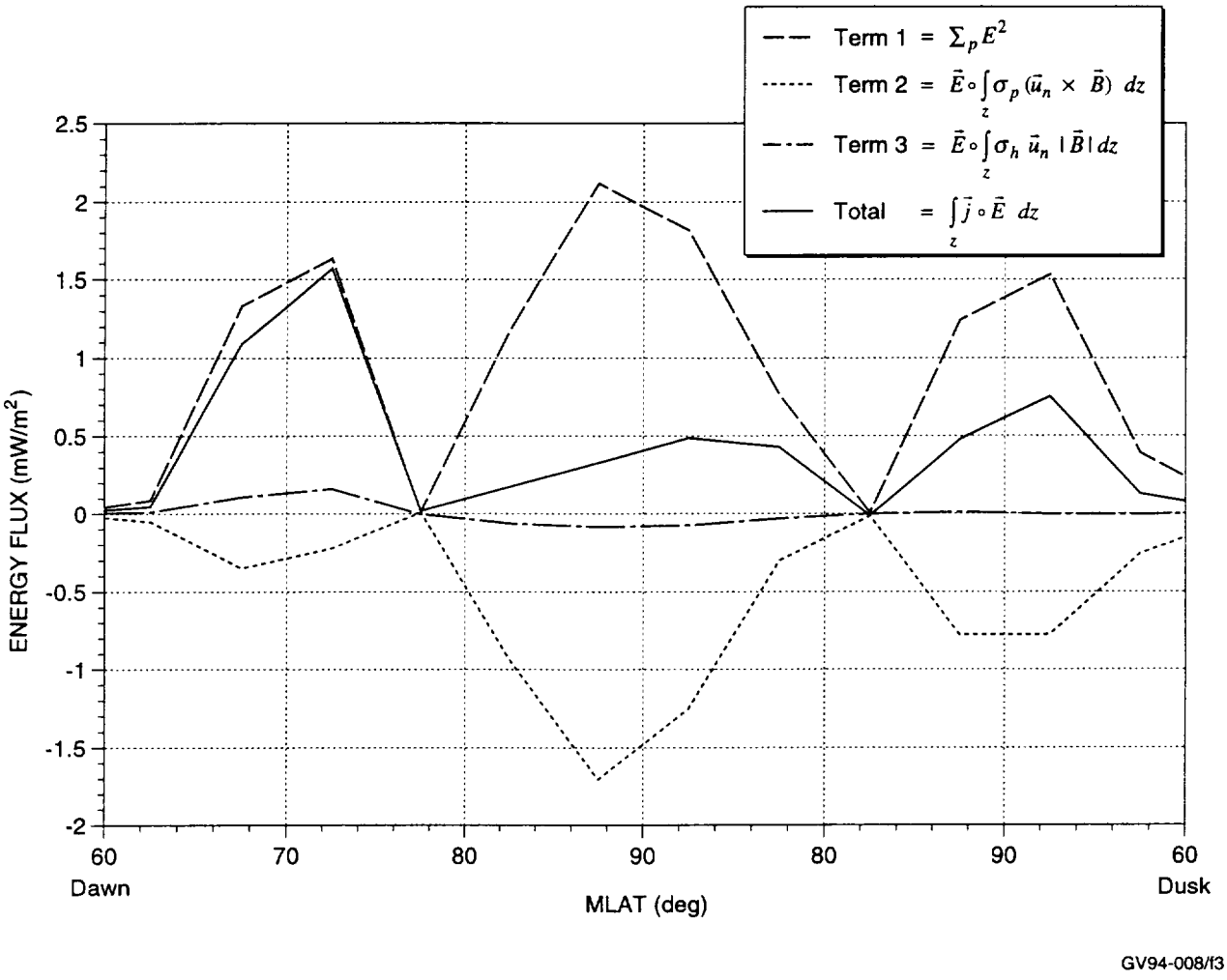

Fig. 3. Height-integrated terms given in Equation 8 along the dawn-dusk magnetic plane in units of mW/m^2.

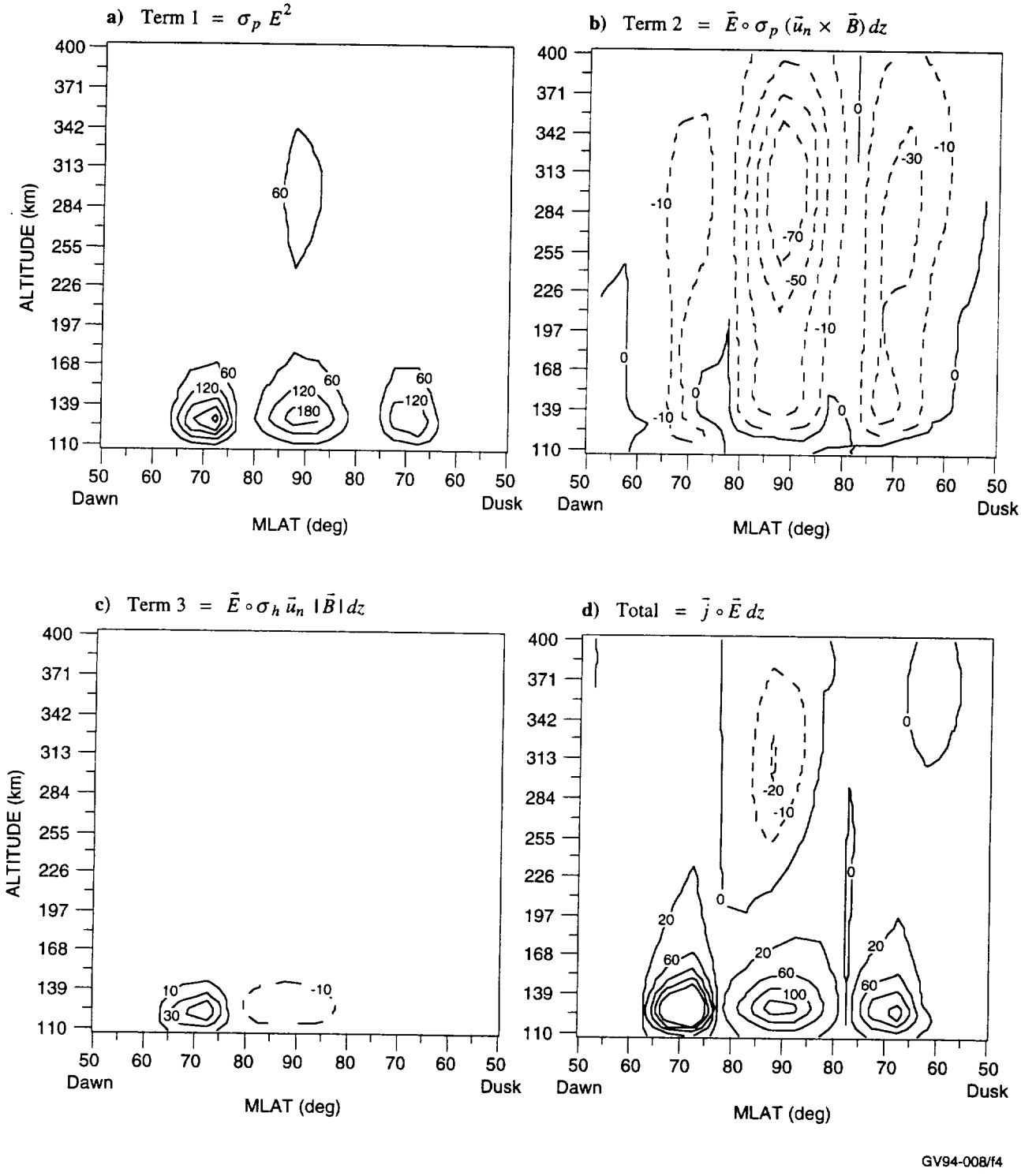

Fig. 4. Altitude distribution for each of the terms in Equation 8 along the dawn-dusk magnetic plane in units of 10^{-7} mW/m^3.

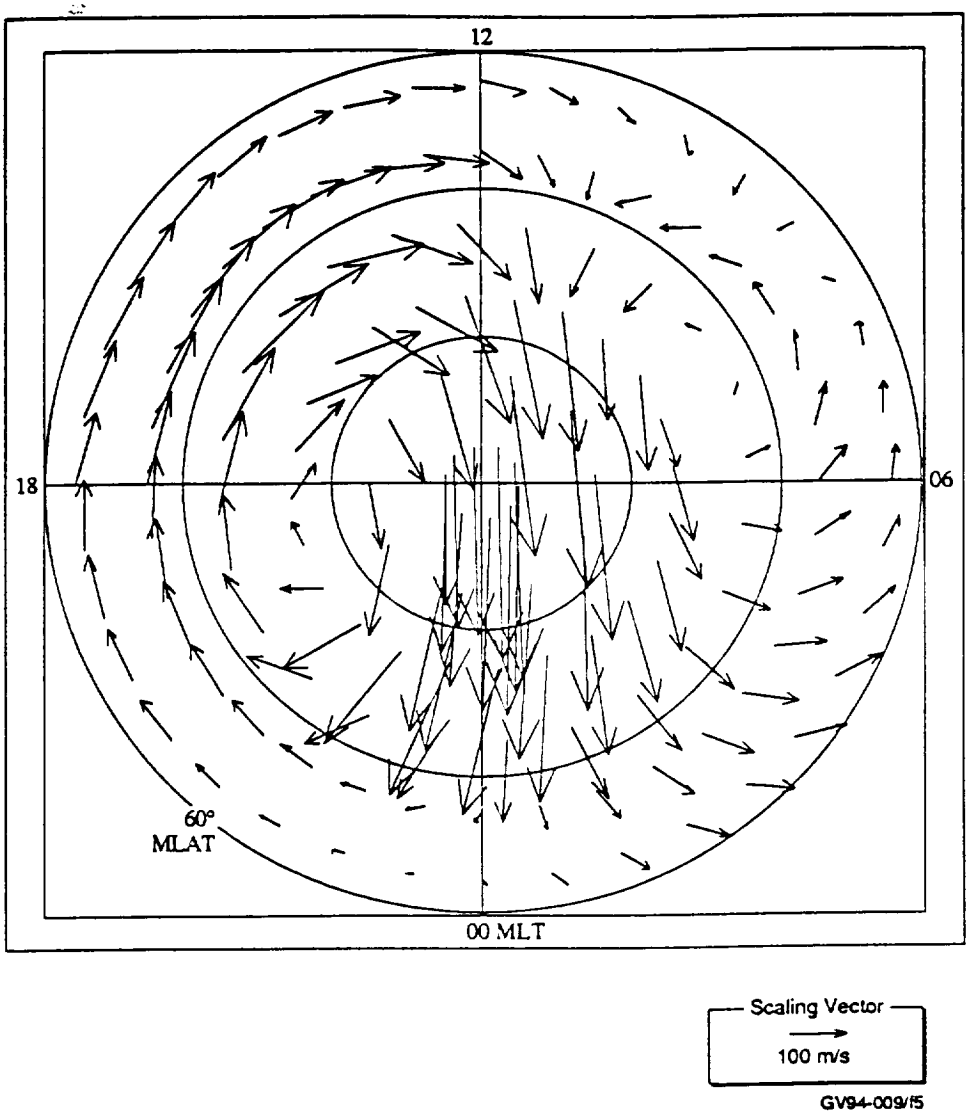

Fig. 5. Polar plot of the effective neutral wind (same format as Figure 2).

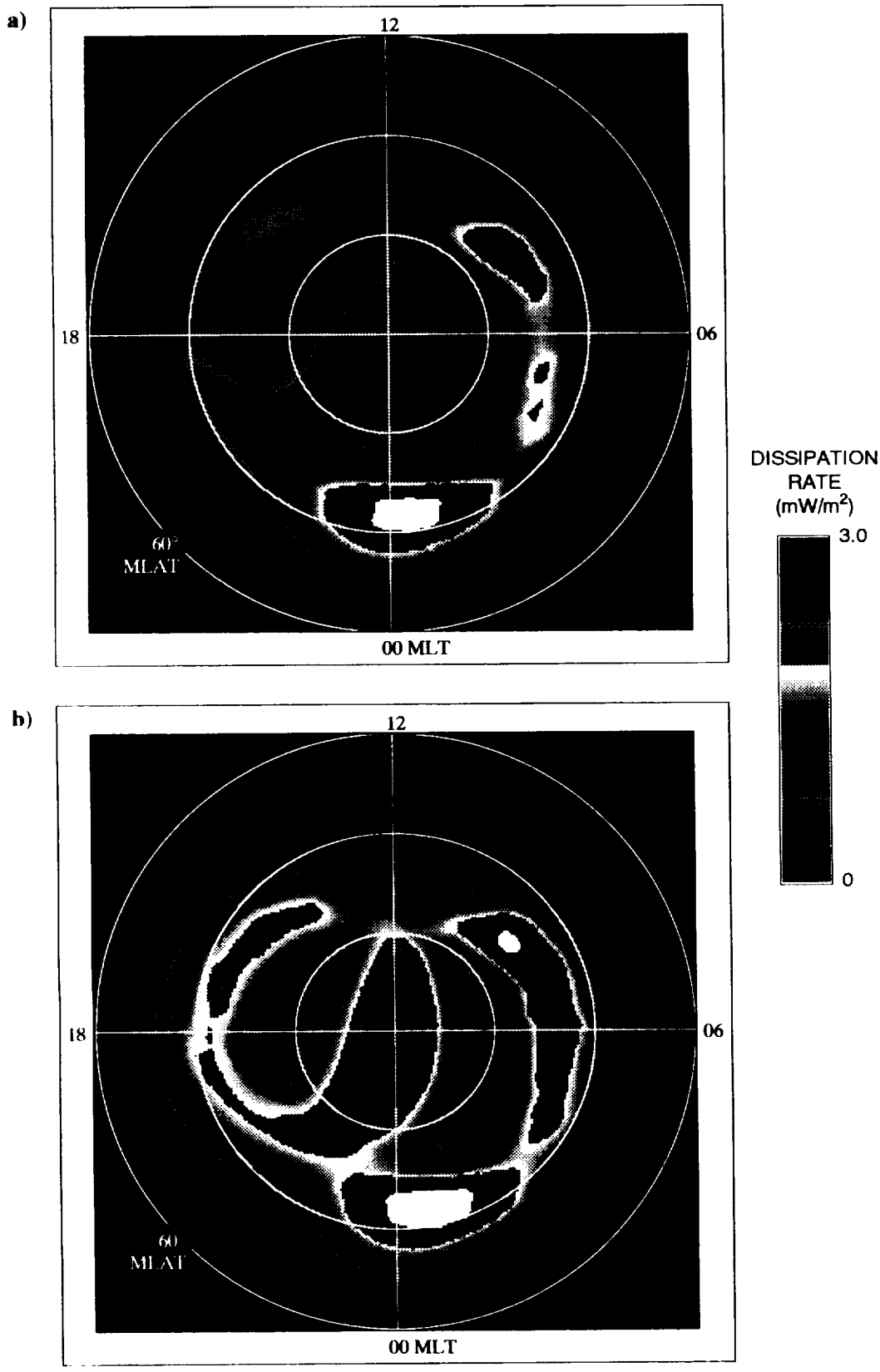

Fig. 6. Polar plots of a) the height-integrated Joule heating rate with neutral winds and b) height-integrated Joule heating rate without neutral winds (same format as Figure 2).

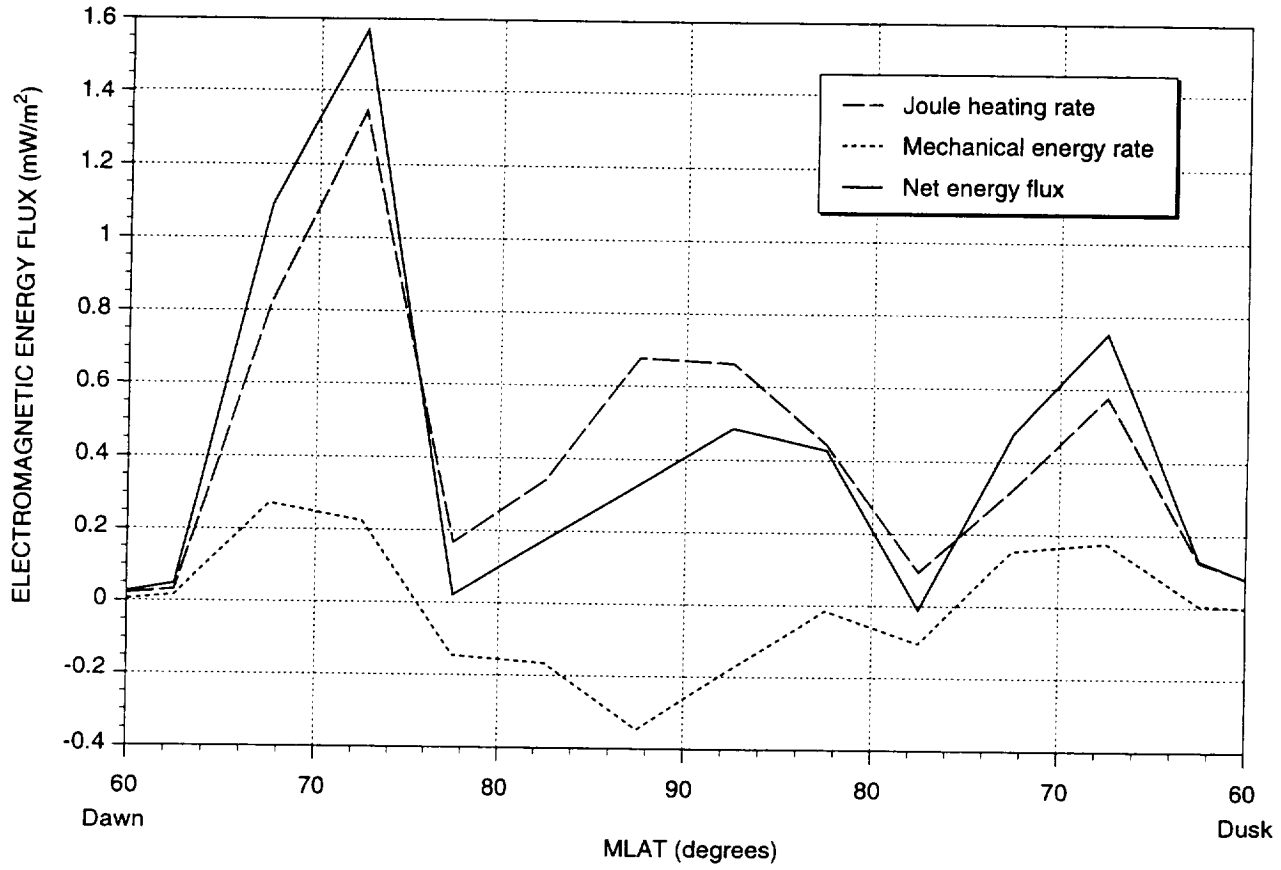

Fig. 7. Height-integrated mechanical energy transfer rate, Joule heating rate, and total electromagnetic energy flux along the dawn-dusk magnetic plane (same format as Figure 3).

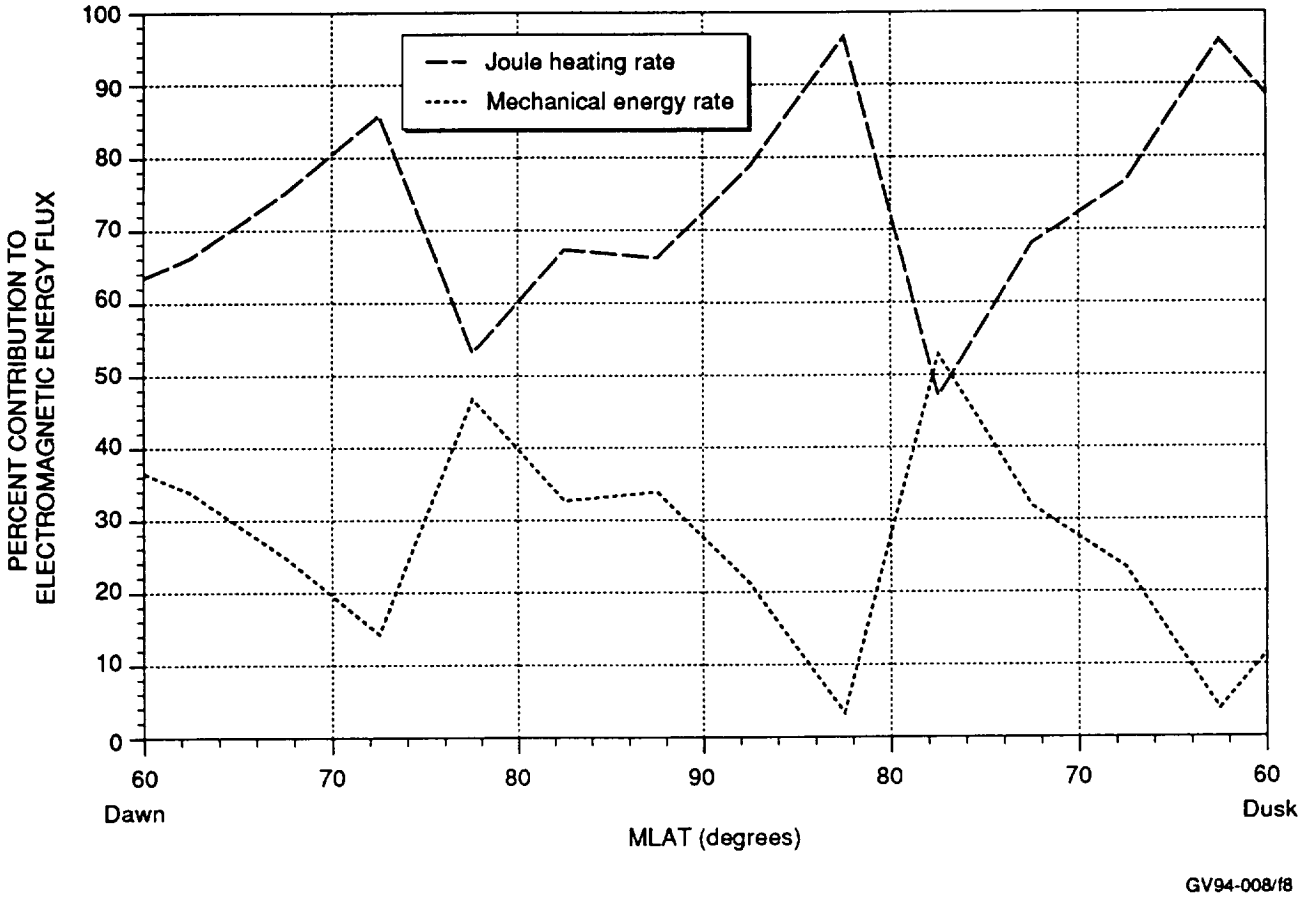

Fig. 8. Percent contribution from the Joule heating rate and the mechanical energy transfer rate to the net electromagnetic energy flux.

Summary of Field-Aligned Poynting Flux Observations from DE 2

J. B. Gary [1] and R. A. Heelis
University of Texas at Dallas, Richardson

J. P. Thayer
SRI International, Menlo Park, California

Received _____; accepted _____

To appear in the *Geophysical Research Letters*, 1994.

Short title:

---

[1]Now at Applied Physics Laboratory, Laurel, Maryland.

Abstract. Using DE 2 data of ion drift velocities and magnetic fields, we have calculated the field-aligned Poynting flux ($S_{\parallel}$) for 576 orbits over the satellite lifetime. This represents the first broad application over an extended data set of Poynting flux observations from *in situ* measurements. This data has been sorted by interplanetary magnetic field conditions (northward or southward IMF) and geomagnetic activity (Kp$\leq$3 and Kp >3) and binned by invariant latitude and magnetic local time. Our general results may be summarized as 1) the averaged $S_{\parallel}$ is everywhere directed into the ionosphere, indicating that electric fields of magnetospheric origin generally dominate, and 2) the distribution of $S_{\parallel}$ for southward IMF can be well explained in terms of an average two cell convection pattern, while for northward IMF a four cell convection pattern may be inferred. We have addressed the interesting question of the distribution of upward Poynting flux by binning only upward observations and found that average upward Poynting flux of less than 3 mW/m^2 may occur anywhere across the high latitude ionosphere. We have also observed a region at high latitudes in the predawn sector where the average upward Poynting flux is of significant size and occurrence frequency during southward IMF and high Kp conditions. This region corresponds to a feature modeled by *Thayer and Vickrey* [1992] and indicates that a neutral wind dynamo may dominate the magnetospheric generator where field lines extend deep into the magnetotail.

Introduction

Several studies of large scale energy dissipation in the high latitude ionosphere have been conducted in the past. They have either involved radar observations [e.g., Vickrey *et al.*, 1982 and included references] or satellite measurements [e.g., Heelis and Coley 1988, Foster *et al.*, 1983] of plasma densities and electric fields together with models of the height-integrated conductivities to estimate the Joule heating rate, $\Sigma_P E^2$, where Σ_P is the height-integrated Pedersen conductivity and E is the electric field in the ionosphere. The use of field-aligned Poynting flux ($S_{\parallel}$) derived from satellite observations of electric fields and perturbation magnetic fields as proposed by Kelley *et al.* [1991] has recently been added as a method for determining the total large scale energy conversion, or transfer, rate $\mathbf{E}\cdot\mathbf{J}$ in the ionosphere. Thayer and Vickrey [1992] and Deng *et al.* [1993] have recently used models of thermospheric circulation to estimate the magnitude of the electromagnetic energy generated by neutral wind dynamo actions and have related this to possible observations of the Poynting flux.

There are two advantages to using $S_{\parallel}$ over electric field and energetic particle observations that are related to the inclusion of neutral wind effects and an independence from modeled conductivities. Computations of the Joule heating rate cannot take into account the height-integrated effects of the difference in ion drift and neutral wind motions [e.g., Banks, 1977, Heelis and Coley, 1988] whereas the Poynting flux is directly dependent on this parameter [Kelley *et al.*, 1991]. Accounting for the motion of the neutral winds is of increasing significance as the electric field becomes smaller than about 10 mV/m [Banks, 1977]. Also, since $S_{\parallel}$ gives an indirect estimate of $\int \mathbf{E}\cdot\mathbf{J}\, dV$ rather than explicitly calculating $\Sigma_P E^2$, it avoids the use of semi-empirical models for Σ_P . A comparison between modeled Joule heating rates and Poynting flux measurements for a single DE 2 orbit has been presented by Deng *et al.* [1991].

In a previous work [Gary *et al.*, 1991], we have described our technique for determining $S_{\parallel}$ from DE 2 observations of the ion drift velocity (V) and perturbation

magnetic field (δB). We also noted in that paper that **E·J** is largely a measure of the height integrated difference between the ion drift velocity and the neutral wind velocity **U**, which is determined by the relative strengths and directions of the different driving mechanisms for **V** and **U**. The velocity difference **V-U** is weighted by the ionospheric conductivity in this height integral. The difficulties in obtaining coordinated observations of neutral winds at different altitudes limits the opportunities for a direct determination of the altitude profile of **V-U**, and further modeling efforts will be required to answer questions regarding the altitude profile of **E·J** .

Data Presentation

Of the several thousand orbits during the satellite lifetime, only about 1300 passes over the high latitude region are available which are suited to our purposes. Determination of $S_{\parallel}$ requires near continuous data between middle latitudes ($\Lambda \leq 50$ deg.) on each side of a high latitude crossing in order to establish a perturbation magnetic field baseline as described in Gary *et al.* [1994]. In addition to this requirement, we have inspected each pass to ensure that the final calculation of $S_{\parallel}$ is made using reliable data. Unreliable measurements of the ion velocity can result from low ion concentrations ($<10^4/cm^3$) producing poor signal to noise ratios in data from the retarding potential analyzer/ion drift meter instrument combination. Sudden shifts in the spacecraft orientation can both alter the baseline for the perturbation magnetic field and introduce spurious signals which result in questionable estimates of the Poynting vector. Orbits which exhibited any of these characteristics have been removed from the data. Ultimately, 576 passes met our criteria for the production of reliable $S_{\parallel}$. These orbits range over all DE 2 altitudes, from about 300 km to 1000 km. As described by Heelis and Coley [1988], the 90 deg. inclination orbit of the DE 2 satellite causes coverage of season to be linked to the local time coverage with dawn-dusk passes occurring predominantly in summer/winter and noon-midnight passes near the equinoxes. It

should also be mentioned that the lifetime of DE 2 occurred during a period of very high solar activity. Interpretations of our data need to be made with these points in mind.

We have binned the data by invariant latitude (Λ) and magnetic local time (MLT) and sorted according to Kp and IMF B_z conditions when possible. Each bin covers 5 deg in Λ and 1 hour in MLT. Kp sorting separates low geomagnetic activity ($0<Kp\leq3$) and high activity ($Kp>3$), and IMF sorting separates northward from southward IMF. The results are shown in polar dials representing the high latitude region above 50 deg invariant latitude using a color coded intensity scale to indicate the magnitude of $S_{\parallel}$. Bins which contain diamonds represent regions where we have less than 75 observations, which we have taken to be the limit for undersampling. The choice of 75 as a limit ensures that at least two passes are included, as one pass may contribute as many as 70 observations in a single bin. Bins which have no shading and no diamond represent regions for which we have no observations. IMF data is available for only 302 of the 576 orbits used in this study, thus reducing the statistics considerably when we examine the distributions under different IMF and Kp conditions. In this work we will continue to use the sign convention where downward directed Poynting flux is negative ($S_{\parallel} < 0$) and indicates electromagnetic energy being converted into particle kinetic energy in the flux tube below the satellite, and upward Poynting flux ($S_{\parallel} > 0$) indicates the generation of electromagnetic energy below the satellite.

Observations for all IMF

The results of our binning procedure for all IMF and Kp conditions are presented in Figure 1. Our results for all combinations of northward/southward IMF with high/low Kp, as well as the corresponding electric field and perturbation magnetic field data, will not be shown in this paper although we will discuss these results when appropriate. The averaged $S_{\parallel}$ is everywhere downward with the largest values occurring near dusk, dawn, and local noon. The highest energy transfer rates are observed between 65 and

80 deg invariant latitude. These regions are generally colocated with the auroral zone, indicating that on average most of the Birkeland currents close locally in region 1/region 2 current sheet pairs. It is easily seen in Figure 1 that the total energy transferred into the ionosphere is greater on the dayside of the dawn-dusk meridian than on the nightside. For the variety of IMF and Kp conditions which we have investigated, the dayside integrated values exceed the nightside values by 20% to 50%.

Across the dayside between 70 and 85 deg there is a region of relatively large $S_{\parallel}$. Part of this region can be associated with cusp currents as well as with the average convection patterns. A region of high average electric field was observed in our results near 70 deg between 0900 MLT and 1200 MLT. This overlaps a region of enhanced magnetic field perturbation producing the "cusp" signature in $S_{\parallel}$ at the same location. There is a bay of smaller valued $S_{\parallel}$ in the premidnight sector which corresponds to relatively small values of $\mathbf{E}$ and $\delta\mathbf{B}$ in the premidnight hours. The premidnight sector showed consistently lower values of $S_{\parallel}$ throughout our analysis, for all IMF and Kp conditions. Comparison between some of the published studies on ion drifts [Kelley, 1989, and included references] and neutral winds [McCormac *et al.*, 1991, Kelley, 1989] as well as model results [e.g., Thayer and Killeen, 1993] indicate that the general circulation of the ions and the neutrals is quite similar in this region. For low Kp, the same asymmetries about the noon-midnight and dawn-dusk meridians exist as for high Kp, but the magnitudes of both $\mathbf{E}$ and $\delta\mathbf{B}$, and thus $S_{\parallel}$, are smaller. The low Kp distribution of $S_{\parallel}$ is dominated by the region of elevated activity near noon. The auroral zone is well defined across the nightside in the $S_{\parallel}$ data as a narrow belt between 65 and 70 deg.

We may compare these results with the similar work of Foster *et al.* [1983] and Heelis and Coley [1988]. The AE C data used by Foster *et al.* was taken at near solar minimum conditions, which makes our study a nice compliment but also makes comparisons somewhat more difficult. We have not attempted to sort our data by season due to the

spacecraft inclination, as stated earlier. Comparison of the electric field data from our work, that of Heelis and Coley, and that of Foster *et al.* reveals general agreement for the large scale distribution. Yet, there is some diversity in the results on energy transfer for similar conditions between the three studies. Our results for all IMF and high Kp indicate the region of greatest activity to be from about 0400 to 1300 MLT, with another belt between 1600 and 1900. Assuming that one could simply sum up Foster *et al.*'s four seasons for high Kp, we would deduce that the greatest activity takes place between about 0800 and 2000 MLT. Heelis and Coley, on the other hand, suggest that the greatest energy dissipation takes place in the regions near midnight and dawn with little activity between noon and 1800 MLT. These differences are largely attributable to the distributions of Σ_P used in the different studies. Foster *et al.* obtained their estimate of Σ_P using the model of Spiro *et al.* [1982] together with energetic particle data to determine the contribution due to precipitating particles, and added to that the solar UV contribution based upon the equation from Mehta [1978]. Heelis and Coley used the same model for Σ_P but with the average inputs for precipitating particles provided by Spiro *et al.* rather than using the measurements from DE 2.

Observations for northward and southward IMF

Figures 2(a) and 2(b) show the results of our sorting the data by the sign of IMF B_z and for high and low Kp, with Figure 2(a) showing the case of southward IMF at high Kp and Figure 2(b) the case of northward IMF at low Kp. Many features of the distribution of $S_{||}$ can be fairly easily reconciled with typical convection patterns associated with northward and southward IMF, and the values at high Kp can be generally described as being larger than, and located at lower latitudes from, those at low Kp. For southward IMF, the average $S_{||}$ exhibits elevated values along the dusk and dawn convection boundaries, or auroral zones, reaching a maximum of about 12 mW/m^2 as seen in Figure 2(a). Note also a region of enhanced $S_{||}$ extending to higher

latitudes between 1000 and 1200 MLT. This region, previously identified with enhanced electric fields in the cusp, is more easily identified when the orientation of the IMF is included in the data selection. The largest bin average is between 1500-1600 MLT and 60-65 deg, and is primarily composed of five southern hemisphere orbits that occurred during magnetic storms. Deng *et al.* [1993] described some of these orbits in their study of the response of the neutral atmosphere to geomagnetic storms. The bin averaged $S_{\parallel}$ is quite large above 60 deg invariant latitude, peaking between 65 and 75 deg.

The interaction between the IMF and geomagnetic field for northward IMF leads to much weaker driving of the ions from magnetospheric electric fields. The northward IMF results in Figure 2(b) shows little variation below 70 deg, indicating that the height-integrated difference between **V** and **U** is relatively small. The largest values are about 7.3mW/m^2 and occur across the dayside in the regions where typical four-cell convection patterns might exist and the general motion of the ions would oppose that of the neutrals. The regions of $S_{\parallel}$ above the background near dawn and dusk are also consistent with a four-cell convection pattern.

Observations of upward Poynting flux

Several authors have addressed the ability of neutral wind motion to generate electromagnetic energy in the lower ionosphere. This energy would be transported along magnetic field lines into the magnetosphere. As discussed in e.g., Kelley *et al.* [1991], this would result in observations of upward $S_{\parallel}$. We have not observered any locations in the high-latitude ionosphere which exhibited upward Poynting flux over a relatively long term average. However, we have taken all observations of upward $S_{\parallel}$ and performed the same binning and sorting of the data as was applied to the overall observations in order to report on the distribution and occurrence of upward Poynting flux. Some of these results are presented in Figure 3. Perhaps the most obvious point to be made from the figure is that the average magnitude of upward Poynting flux is quite small under

all conditions, with no single bin greater than 2.25 mW/m^2 . Such small average values are in line with the modelling of Thayer and Vickrey [1992] and Deng *et al.* [1993]. All of our observations above the nominal uncertainty level of 0.5 mW/m^2 occur above 65 deg. invariant latitude.

Figure 3 depicts the distribution of upward $S_{||}$ for all IMF and high Kp. The largest bin averages occur on the dawnside of the noon-midnight meridian, and are almost entirely composed of southward IMF observations. On the duskside, the occurrences are of smaller magnitude and seem to be sporadically located. There are no significant observations above 85 deg, few below 65 deg, and observations of upward $S_{||}$ near noon are noticeably absent. For low Kp, observations of substantial ($> 1 mW/m^2$) upward $S_{||}$ averages all but vanish. The early morning hours which show the largest upward $S_{||}$ at high Kp exhibit insignificant average values at low Kp.

It is apparent that, while observations of upward $S_{||}$ occur over most of the high latitude ionosphere, they are not widely significant in an average sense. Bin averages greater than 0.5 mW/m^2 are rare, and it is possible that most could vanish if a substantially larger data set was employed. A likely exception would be the region between 70-80 deg near 0300 MLT. We have examined the frequency of occurrence of upward $S_{||}$ greater than 0.5 mW/m^2 , and in this region it exceeds 20% for southward IMF. The occurrence frequency is determined by taking the ratio of the number of observations for which $S_{||} > 0.5$ mW/m^2 to the total number of observations in each bin. Detailed examination of the binned orbits in this region does not suggest that the upward Poynting flux observations are suspect. Few regions show an occurrence frequency greater than 10%, but even this frequency is somewhat remarkable. Examination of separate orbits reveals that the regions of appreciable upward Poynting flux are associated with field-aligned currents in the polar cap which are distinctly smaller in scale size than the large scale region 1 and region 2 current distributions. Such field-aligned currents are likely to arise from divergences in the horizontal ionospheric

currents which should exist whenever the thermospheric winds become the dominant driver of electromagnetic energy.

We could perhaps have predicted the existence of this region of upward Poynting flux by considering the electrical connection between the ionosphere, magnetosphere, and solar wind, together with the bulk motion of the ions and neutrals in the predawn polar cap. The field lines connecting the predawn ionosphere to the magnetosphere and beyond during southward IMF extend far into the magnetotail, where the magnetosheath plasma is super-Alfvenic. This argues for a weak connection along open field lines between the magnetospheric electric field driver and the ionospheric load. In addition, the neutral gas obtains its highest velocities during southward IMF and high Kp conditions in just this region. The combination of relatively rapid moving neutral particles traveling in the same direction as weakly magnetospheric driven ions is exactly the requirement for a significant large scale neutral wind dynamo. In their work on assessing the role of the neutral wind dynamo in high latitude energy generation, Thayer and Vickrey [1992] predicted this general location to be dominated by the neutral wind.

Conclusion

Our work in determining the distribution of the energy transfer rate in the high latitude ionosphere using observations of the field-aligned Poynting flux $S_{\parallel}$ has produced the following results:

1) $S_{\parallel}$ is downward everywhere on average;

2) for southward IMF, a two-cell convection pattern is evidenced with the greatest $S_{\parallel}$ occurring in the auroral zones at dawn and dusk, with an "offset" cusp region at higher latitudes just before noon;

3) for northward IMF, a four-cell convection pattern is evidenced with the greatest $S_{\parallel}$ occurring near noon where we might expect the ion and neutral gas bulk flows to have opposite directions;

4) upward Poynting flux may be observed at all locations but at generally small values, averaging to less than 1 mW/m^2 , and never with sufficient frequency to dominate a long term average;

5) there is a region of significant upward Poynting flux generated in the predawn polar cap with an average of greater than 2 mW/m^2 , although the net $S_{||}$ is downward when all observations are averaged. Observations of upward $S_{||}$ account for more than 20% of the total observations for southward IMF with Kp>3 in this region;

This work is supported at the University of Texas at Dallas by SRI International subcontract C-M0608 and by Air Force Geophysics Directorate contract F19628-93-K-0008.

Figure 1. Polar dial showing the distribution of the average field-aligned Poynting flux ($S_{\parallel}$) in magnetic local time (MLT) and invariant latitude (A) above A=50°. The bins used in the averaging cover 1 hour in MLT and 5 degrees in A. The data are for all IMF orientations and Kp values, averaged over 570 DE 2 high latitude passes.

Figure 2. Results of sorting the bin averaged $S_{\parallel}$ data by southward and northward IMF for high and low Kp, in the same format as Figure 1 but with a different scale. Bins with no data are not colored. Bins with fewer than 75 measurements are shown with a diamond. (a) results for southward IMF and Kp>3, representing data from 92 high latitude passes. (b) results for northward IMF and Kp<3, representing data from 117 passes.

Figure 3. Results of the bin averaged upward Poynting flux in the same format as Figure 1. Only measurements of $S_{\parallel}$ >0 have been included in the averages, for Kp>3.

References

Banks, P. M., Observations of Joule and particle heating in the auroral zone, *J. Atmos. Terr. Phys.*, *39*, 179, 1977.

Deng, W., T. L. Killeen, A. G. Burns, R. G. Roble, J. A. Slavin, and L. E. Wharton, The effects of neutral inertia on ionospheric currents in the high latitude thermosphere following a geomagnetic storm, *J. Geophys. Res.*, *98*, 7755-7790, 1993.

Deng, W., T. L. Killeen, A. G. Burns, R. M. Johnson, B. A. Emery, R. G. Roble, J. D. Winningham, and J. B. Gary, A one-dimensional hybrid satellite model for the Dynamics Explorer 2 (DE 2) satellite, *J. Geophys. Res.*, in press.

Foster, J. C., J.-P. St-Maurice, and V. J. Abreu, Joule heating at high latitudes,*J. Geophys. Res.*, *88*, 4885-4896, 1983.

Gary, J. B., R. A. Heelis, W. B. Hanson, and J. A. Slavin, Field-aligned Poynting flux observations in the high latitude ionosphere, *J. Geophys. Res.*, *99*, 11417-11427, 1994.

Heelis, R. A., and W. R. Coley, Global and local Joule heating effects seen by DE 2, *J. Geophys. Res.*, *96*, 7551-7557, 1988.

Kelley, M. C., *The Earth's Ionosphere*, Academic Press, New York, 1989.

Kelley, M. C., D. J. Knudsen, and J.F. Vickrey, Poynting flux measurements on a satellite: A diagnostic tool for space research., *J. Geophys. Res.*, *96*, 201-207,1991.

McCormac, F. G., T. L. Killeen, and J. P. Thayer, The influence of IMF B_y on the high-latitude thermospheric circulation during northward IMF, *J. Geophys. Res.*, *96*, 115-128,1991.

Spiro, R. W., P. H. Reiff, and J. L.J. Maher, Precipitating electron energy flux and auroral zone conductances, An empirical model, *J. Geophys. Res.*, *87*, 8215-8227, 1982.

Thayer, J. P., and T. L. Killeen, A kinematic analysis of the high-latitude thermospheric neutral circulation pattern, *J. Geophys. Res.*, *98*, 11,549-11,565, 1993.

Thayer, J. P. and J. F. Vickrey, On the contribution of the thermospheric neutral wind to high-latitude energetics, *Geophys. Res. Lett.*, *19*, 265, 1992.

Vickrey, J. F., R. R. Vondrak, and S. J. Matthews, Energy deposition by precipitating particles and Joule dissipation in the auroral ionosphere, *J. Geophys. Res.*, *87*, 5184-5196, 1982.

This manuscript was prepared with the AGU LaTeX macros v3.0.